Journal of Applied Physics

Contributions to polarization and polarization switching in antiphase boundaries of $SrTiO_3$ and $PbZrO_3$ EP

Cite as: J. Appl. Phys. **128**, 194101 (2020); https://doi.org/10.1063/5.0030038
Submitted: 21 September 2020 . Accepted: 02 November 2020 . Published Online: 17 November 2020

W. Schranz, A. Tröster, and I. Rychetsky

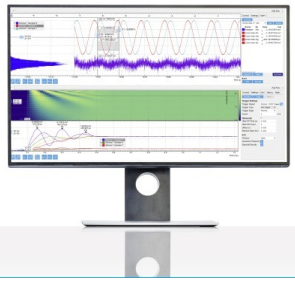

AIP Publishing

Journal of Applied Physics ARTICLE scitation.org/journal/jap

Contributions to polarization and polarization switching in antiphase boundaries of $SrTiO_3$ and $PbZrO_3$

Cite as: J. Appl. Phys. **128**, 194101 (2020); doi: 10.1063/5.0030038
Submitted: 21 September 2020 · Accepted: 2 November 2020 ·
Published Online: 17 November 2020

W. Schranz,[1,a] A. Tröster,[1] and I. Rychetsky[2]

AFFILIATIONS

[1]University of Vienna, Faculty of Physics, Boltzmanngasse 5, 1090 Wien, Austria
[2]Institute of Physics, Academy of Sciences of the Czech Republic, Na Slovance 2, 18221 Prague 8, Czech Republic

Note: This paper is part of the Special Topic on Domains and Domain Walls in Ferroic Materials
[a]**Author to whom correspondence should be addressed:** wilfried.schranz@univie.ac.at

ABSTRACT

We use a recently developed method—based on layer group analysis combined with the Landau theory—to investigate the polar properties of antiphase boundaries (APBs) in $SrTiO_3$ and $PbZrO_3$. For $SrTiO_3$, we find that, in addition to the biquadratic, Houchmandazeh-Laizerowicz-Salje (HLS) coupling $b_{ijkl}P_iP_j\phi_k\phi_l$ in the Landau-Ginzburg free energy expansion, additional rotopolar terms of the form $W_{ijkl}P_i\phi_k\frac{\partial\phi_l}{\partial x_j}$ contribute considerably to the polarization of antiphase boundaries in these materials. The rotopolar terms can be split into a symmetric flexoelectric part and an antisymmetric one. The antisymmetric Lifshitz term leads to a macroscopic polarization of APBs, which can be switched by application of an external electric field. For $PbZrO_3$, the observed polarization profiles [Wei *et al.*, Mater. Res. Bull. **62**, 101 (2015)] are fully compatible with the symmetries of the corresponding layer groups. Unlike in $SrTiO_3$, there exists no Lifshitz invariant $W_{ijkl}P_i\eta_k\frac{\partial\eta_l}{\partial x_j}$ for the order parameter $\eta_i(i = 1, \ldots, 12)$ describing the displacements of lead atoms. However, a detailed group theoretical treatment indicates that the polarity of APBs in $PbZrO_3$ is driven by higher order interactions between polarization P_i, order parameter η_k, and order parameter gradients $\frac{\partial\eta_l}{\partial x_j}$.

I. INTRODUCTION

Domain walls (DWs) have attracted much interest due to their ability of carrying functional properties[1–5] that are different from the surrounding bulk. For example, ferroelastic DWs in $SrTiO_3$,[6] $LaAlO_3$,[7] $BiVO_4$,[8] etc. have been shown to be polar. It is generally accepted that the polarization of ferroelastic DWs is due to flexoelectric coupling $f_{ijkl}P_k\frac{\partial u_{ij}}{\partial x_l}$ between polarization P_k and the strain-gradient ∇u_{ij} in a free energy expansion.[9] Such polarization, however, cannot be switched, which makes it less attractive for technical applications. However, recently Schiaffino and Stengel[10] have discovered an interesting symmetry breaking effect in a special (cycloidal) sequence of ferroelastic DWs of $SrTiO_3$. Based on a multiscale first-principle approach, these authors have identified two new coupling mechanisms that contribute to the polarization of ferroelastic DWs in $SrTiO_3$, i.e., a rotopolar coupling between the polarization and gradients of the oxygen octahedron rotations and a trilinear coupling between the polarization P, the oxygen octahedron rotation ϕ, and the displacement u_z of Ti atoms. It turned out that this rotopolar coupling allows for a breakdown of macroscopic inversion symmetry—similar to in cycloidal magnets—which leads to a macroscopic polarization of a special sequence of parallel ferroelastic DWs. Very recently, we have studied[11] the polarization of domain boundaries in $SrTiO_3$ using a combination[12] of layer groups with order parameter (OP) symmetry. We found that the special sequence[10] of ferroelastic DWs produces a net macroscopic polarization that must always contain a mixed ferroelastic DW, i.e., of the orientational/translational type that contains an antiphase boundary (APB). In this way, we unveiled that the rotopolar coupling provides an important mechanism for polarization of translational APBs.

Translational APBs below antiferrodistortive phase transitions are particularly interesting due to their ability to carry DW

polarization.[13] The antiferroelectric crystal $PbZrO_3$ corresponds to the very few cases where there is experimental evidence that APBs are polar.[14,15] Moreover, based on ab initio calculations, the authors of Ref. 14 claimed that the DW polarization can be switched, supporting its ferroelectric nature. Ferroelectric (=polar and switchable) antiphase boundaries could be extremely interesting for nanotechnological applications,[16,17] similar to those which are quickly emerging in the field of antiferromagnetic spintronics.[18]

$SrTiO_3$ is another example for which polarization inside APBs was predicted.[19] In $SrTiO_3$ and $PbZrO_3$,[14] the authors[19] explained the possible appearance of a polarization component P_i in APBs as a result of a local ferroelectric transition below $T_c^* < T_c$ induced by a biquadratic coupling term $bP^2\phi^2$ between the primary order parameter (OP) ϕ and the polarization P in the free energy expansion. In the present work, we show that there is another important coupling mechanism, which crucially contributes to the polarization of APBs. The rotopolar coupling between polarization and gradients of the primary order parameter, which was identified[10] to lead to a macroscopic polarization from antiferrodistortive cycloids in $SrTiO_3$, is shown here to contribute significantly to DW polarization in APBs of $SrTiO_3$ and $PbZrO_3$.

II. RESULTS AND DISCUSSION

A. Antiphase boundaries in strontium titanate

$SrTiO_3$ undergoes an antiferrodistortive structural phase transition[21] at $T_c = 105$ K from a simple cubic room temperature phase with space group $G = Pm\bar{3}m$ to a tetragonal phase $F = I4/mcm$, where $F < G$. The space group of the cubic phase is symmorphic, i.e., $G = \sum_{g\in m\bar{3}m} \mathbf{T}^c(g|000)$, where $\mathbf{T}^c = \{n_1\mathbf{a}_1^c + n_2\mathbf{a}_2^c + n_3\mathbf{a}_3^c\}$ is the translation group with $\mathbf{a}_1^c = (a, 0, 0)$, $\mathbf{a}_2^c = (0, a, 0)$, and $\mathbf{a}_3^c = (0, 0, a)$, with $a = 3.905$ Å. The phase transition is due to static rotations $(0, 0, \phi_3)$ of the TiO_6-octahedra around the tetragonal **c**-axis, which are alternating $(0, 0, \pm\phi_3)$ along all three cubic directions (see Fig. 1 for the present setting). Due to these staggered rotations, the translations $(2n_1 + 1)(a, 0, 0)$, $(2n_2 + 1)(0, a, 0)$, and $(2n_3 + 1)(0, 0, a)$ are lost. The tetragonal lattice is then related to the cubic one (Fig. 1) as $\mathbf{T}^t = \{\mathbf{a}_1^c + \mathbf{a}_2^c, -\mathbf{a}_1^c + \mathbf{a}_2^c, \mathbf{a}_2^c + \mathbf{a}_3^c\} = \{(a, a, 0), (-a, a, 0), (0, a, a)\}$. The phase transition occurs at the R-point, i.e., $\mathbf{k}_R = \frac{2\pi}{a}(\frac{1}{2}\frac{1}{2}\frac{1}{2})$ of the BZ, with the active irrep[11] R_4^+.

Due to the symmetry reduction at the phase transition, the distorted phase can appear in $N = 6$ domain states (DSs), which we designate as $1_1, 1_2, 2_1, 2_2, 3_1, 3_2$, where the first number denotes the three different orientation states 1, 2, 3 and the subscript specifies one of the two different translational states within each orientation state. In Ref. 11, we have analyzed the symmetry and properties of DWs, which connect a variety of domain states (DSs). Here, we will focus on APBs, specifically on translational DWs connecting the DSs 3_1 and 3_2. In $SrTiO_3$, two types of translational DWs are distinguished.[19] For *easy* APBs (Fig. 2), the rotation $(0, 0, \phi_3)$ of the octahedra is parallel to the DW normal **n**, whereas for *hard* APBs (Fig. 3), $(0, 0, \phi_3)$ is perpendicular to **n**. Hard APBs were found[22] to be about 10 unit cells (ca. 40 Å) thick, whereas easy APBs[23] are atomistic thin.

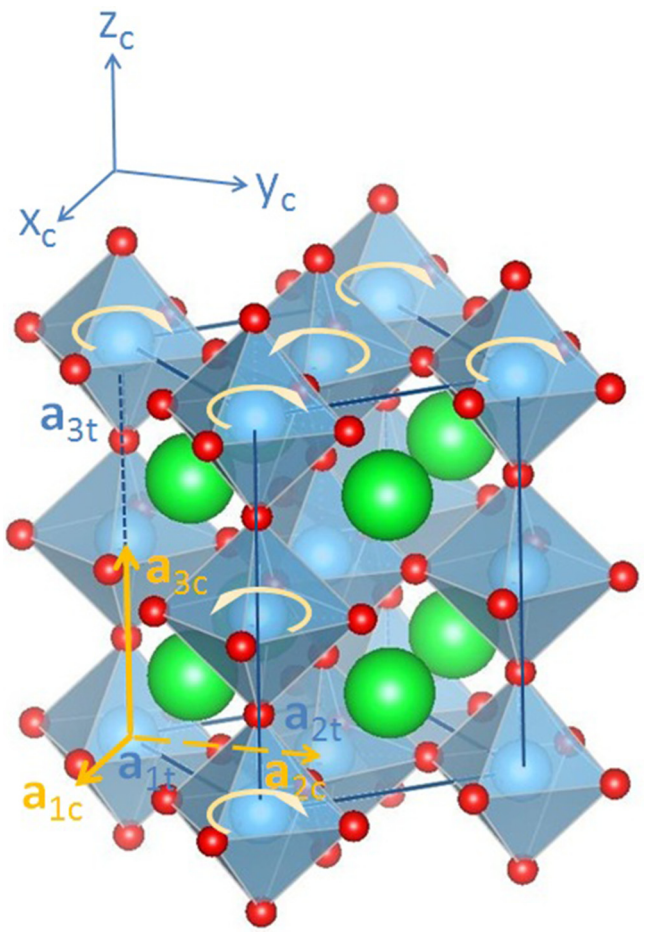

FIG. 1. Structure of $SrTiO_3$. Relation between cubic $Pm\bar{3}m$ and tetragonal $I4/mcm$ unit cells of $SrTiO_3$. Note that we are working entirely in the cubic reference frame, i.e., (x_c, y_c, z_c). Sometimes, we use also the notation (x_1, x_2, x_3). The origin (0, 0, 0) is chosen at Ti atoms (light blue), Sr atoms (green) at $(\frac{a}{2}, \frac{a}{2}, \frac{a}{2})$ and O atoms (red) at $(\frac{a}{2}, 0, 0)$ and equivalent positions. This and similar drawings were made with VESTA.[20]

Since it was shown[19,22] that hard APBs in $SrTiO_3$ are the most promising candidates for carrying a polarization within the wall, we will analyze this case in more detail. In Ref. 11, we found that the layer group symmetry[24] $T_{3_13_2}$ of a domain twin (DT) $(3_1|3_2)$ at the position $\mathbf{p} = (\frac{1}{2}00)$ with $\mathbf{n} = [100]$ is given by the following symmetry elements:

$$T_{3_13_2}(\mathbf{n} = [100], \mathbf{p} = (000)) = \mathbf{T}\{(1/000)\,(2_x/00a)\,(m_y/00a)\,(m_z/000) \times (\hat{2}_y/000)\,(\hat{m}_x/000)\,(\hat{2}_z/00a)\,(\hat{\bar{1}}/00a)\}, \quad (1)$$

where $\mathbf{T} = (0, na, ma)$, $n + m = 2k$.

It is easy to see that the orthorhombic point group ($D_{2h} = mmm$), which corresponds to the layer group $T_{3_13_2}$

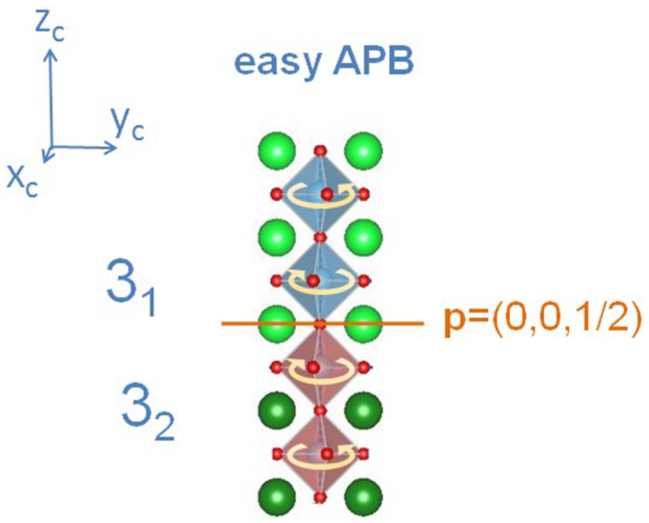

FIG. 2. Easy APB of the Ising type. Schematics of an *easy* APB $(3_1|3_2)$ with $\mathbf{n} = [001]$ in tetragonal $SrTiO_3$ at $\mathbf{p} = (0, 0, \frac{1}{2})$.

of Eq. (1), restricts the polarization components to $P_1(-x_1) = -P_1(x_1)$, $P_2(x_1) = 0$, and $P_3(x_1) = 0$, i.e., does not allow for any polarization component in the center of such a wall. Moreover, in Ref. 11, we found that the symmetry elements (1) constrain the OP-profile to a one-dimensional solution, i.e., $(0, 0, \phi_3) \rightarrow (0, 0, -\phi_3)$ along the path $-\infty \leq x_1 \leq \infty$, which is frequently called an Ising-type solution. Thus, for the case of a one-dimensional OP profile (Ising walls), APBs in $SrTiO_3$ are not expected to carry a polarization. However, since Tagantsev *et al.*[19] have shown that *hard* APBs in $SrTiO_3$ develop (already at $T_c = 105$ K) a component of $\boldsymbol{\phi}$ perpendicular to the boundary plane, similar to Néel walls in magnetic systems, we want to check how the layer group symmetry of Eq. (1) is lowered for the case of $(\phi_1, 0, \phi_3) \rightarrow (\phi_1, 0, -\phi_3)$ along the path $-\infty \leq x_1 \leq \infty$. More precisely, it is assumed that $\phi_1(x_1) = \phi_1(-x_1)$.

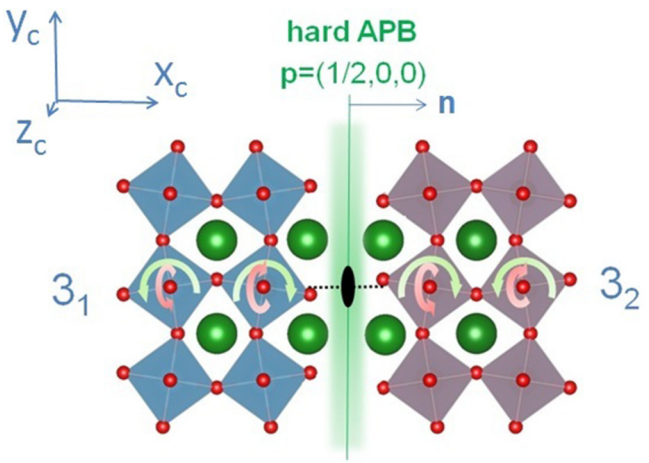

FIG. 3. Hard APB of the Neél type. Representation of a *hard* APB ($\mathbf{n} = [100]$) in tetragonal $SrTiO_3$ at $\mathbf{p} = (\frac{1}{2}, 0, 0)$. Green arrows represent octahedra rotations corresponding to $(0, 0, \phi_3) \rightarrow (0, 0, -\phi_3)$ in the APB. Their phase is shifted by π when going from 3_1 to 3_2. Pink arrows sketch the additional ϕ_1 component, arising for Neél-type solutions.[19] The symmetry elements of the layer group [Eq. (2)], when the symmetry breaking due to $\phi_1 \neq 0$ is taken into account, are depicted in the center of the wall. The mirror planes m_x and m_y allow only for odd polarization components P_x and P_y, but the twofold axis 2_z is compatible with an even polarization distribution $P_z(x)$.

In Ref. 11, we found that due to the appearance of the component ϕ_1 in the wall, the symmetry (1) is lowered to

$$T_{3_1 3_2}(\mathbf{n} = [100], \mathbf{p} = (\frac{1}{2}00)) = \mathbf{T}\{(1/000)\,(m_y/00a)\,(\underline{\hat{m}}_x/00a)\,(\hat{\underline{2}}_z/000)\}, \quad (2)$$

with $\mathbf{T} = (0, na, ma)$, $n + m = 2k$. Thus, the appearance of $\phi_1 \neq 0$ in the vicinity of a hard APB breaks the point group symmetry from $D_{2h} = mmm$ (for $\phi_1 = 0$) to $C_{2v} = mm2$, which allows for the development of the even polarization component $P_3(-x_1) = P_3(x_1)$. The other two components are again constrained by this symmetry to $P_1(-x_1) = -P_1(x_1)$, $P_2(x_1) = 0$, as before. The total polarization of the APB, $\mathcal{P}_i = \langle P_i \rangle \equiv \int_{-\infty}^{\infty} P_i dx_1$, is also of the interest, and in our case $(\mathcal{P}_1, \mathcal{P}_2, \mathcal{P}_3) = (0, 0, \mathcal{P}_3)$, where $\mathcal{P}_3 \neq 0$ is the only nonzero component.

1. Domain wall symmetry and coupling contributions to polarization of APBs in strontium titanate

The commonly accepted explanation for the polarization of APBs arises from a repulsive biquadratic coupling $\propto \boldsymbol{\phi}^2\mathbf{P}^2$ between the primary OP $\boldsymbol{\phi}$ and the polarization $\mathbf{P}$.[19,25] This elegant reasoning works for the case when—like, e.g., in incipient ferroelectrics—the occurrence of the primary OP $\boldsymbol{\phi}$ suppresses the appearance of polarization $\mathbf{P}$. In this case, the mode corresponding to $\boldsymbol{\phi}$ softens at T_c, and due to the $\mathbf{P}^2\boldsymbol{\phi}^2$ repulsion the ferroelectric transition does not occur. However, in an APB, the OP can change from $\phi(x)$ to $-\phi(x)$ via $\phi = 0$ in the DW center. Thus, in such a simplified picture, the repulsion is completely suppressed, and a ferroelectric transition can occur in the center of the DW.

In $SrTiO_3$, it was shown that this coupling leads to a polarization of APBs below $T_c^* \approx 40$ K, which corresponds roughly to the instability temperature of the ferroelectric phase that is suppressed by the appearance of the structural phase transition at $T_s \approx 105$ K. This coupling yields an symmetric polarization distribution $P_3(x)$ (see, e.g., Ref. 22) with a maximum at the DW center. Moreover, such induced polarization can be switched by application of an external electric field, thus making it extremely interesting for potential applications. In a recent work, however, Schiaffino and Stengel[10] discovered that in a special (cycloidal) sequence of ferroelastic twins a macroscopic polarization can arise. In our notation, such a sequence corresponds to an orientational domain twin, e.g., $(1_1|2_1)$ followed by a mixed orientational/translational twin $(2_1|1_2)$. In Ref. 10, a direct rotopolar coupling between polarization and the

gradients of the oxygen octahedra tilts was shown to contribute crucially to the macroscopic polarization. Using the irreducible representation $R_4^+(\phi_1, \phi_2, \phi_3)$, the complete set of rotopolar couplings[11] takes the form

$$\begin{aligned} F = F_L &+ W_1\left[P_1\left(\frac{\partial\phi_1}{\partial x_3}\phi_3 + \frac{\partial\phi_1}{\partial x_2}\phi_2\right) + P_2\left(\frac{\partial\phi_2}{\partial x_3}\phi_3 + \frac{\partial\phi_2}{\partial x_1}\phi_1\right) + P_3\left(\frac{\partial\phi_3}{\partial x_1}\phi_1 + \frac{\partial\phi_3}{\partial x_2}\phi_2\right)\right] \\ &+ W_2\left[P_1\left(\frac{\partial\phi_2}{\partial x_2}\phi_1 + \frac{\partial\phi_3}{\partial x_3}\phi_1\right) + P_2\left(\frac{\partial\phi_1}{\partial x_1}\phi_2 + \frac{\partial\phi_3}{\partial x_3}\phi_2\right) + P_3\left(\frac{\partial\phi_1}{\partial x_1}\phi_3 + \frac{\partial\phi_2}{\partial x_2}\phi_3\right)\right] \\ &+ W_3\left[P_1\left(\frac{\partial\phi_3}{\partial x_1}\phi_3 + \frac{\partial\phi_2}{\partial x_1}\phi_2\right) + P_2\left(\frac{\partial\phi_3}{\partial x_2}\phi_3 + \frac{\partial\phi_1}{\partial x_2}\phi_1\right) + P_3\left(\frac{\partial\phi_1}{\partial x_3}\phi_1 + \frac{\partial\phi_2}{\partial x_3}\phi_2\right)\right] \\ &+ W_4\left[P_1\frac{\partial\phi_1}{\partial x_1}\phi_1 + P_2\frac{\partial\phi_2}{\partial x_2}\phi_2 + P_3\frac{\partial\phi_3}{\partial x_3}\phi_3\right]. \end{aligned} \tag{3}$$

In Ref. 11, we have analyzed the above-mentioned sequence $(1_1|2_1|1_2)$, showing that the macroscopic polarization must be related to the extra polarization in the APB, which appears in the mixed ferroelastic DW. Here, we show how the rotopolar coupling contributes to the polarization of the present APB $(3_1|3_2)$, with $n = [100]$. For this case, the relevant terms in Eq. (3) can be reduced to

$$\begin{aligned} F = F_L &+ P_1\left(W_3\frac{\partial\phi_3}{\partial x_1}\phi_3 + W_4\frac{\partial\phi_1}{\partial x_1}\phi_1\right) \\ &+ P_3\left(W_1\frac{\partial\phi_3}{\partial x_1}\phi_1 + W_2\frac{\partial\phi_1}{\partial x_1}\phi_3\right). \end{aligned} \tag{4}$$

In the following, we show qualitatively how these couplings contribute to the polarization components of the present APB and how the polarization profiles correlate with the layer group symmetry of the twin.

Let us start with the general properties of $(3_1|3_2)$ APB derived from Eq. (4). Minimizing the free energy, we get

$$\begin{aligned} P_1 \propto \left(W_3\frac{\partial\phi_3}{\partial x_1}\phi_3 + W_4\frac{\partial\phi_1}{\partial x_1}\phi_1\right) = \frac{1}{2}\left(W_3\frac{\partial(\phi_3\phi_3)}{\partial x_1} + W_4\frac{\partial(\phi_1\phi_1)}{\partial x_1}\right), \\ P_3 = P_3^{flexo} + P_3^{Lifshitz} \propto \left(W_1\frac{\partial\phi_3}{\partial x_1}\phi_1 + W_2\frac{\partial\phi_1}{\partial x_1}\phi_3\right), \end{aligned} \tag{5}$$

where

$$\begin{aligned} P_3^{flexo} &\propto \frac{1}{2}(W_1 + W_2)\left(\frac{\partial\phi_3}{\partial x_1}\phi_1 + \frac{\partial\phi_1}{\partial x_1}\phi_3\right) = \frac{1}{2}(W_1 + W_2)\left(\frac{\partial(\phi_3\phi_1)}{\partial x_1}\right), \\ P_3^{Lifshitz} &\propto \frac{1}{2}(W_1 - W_2)\left(\frac{\partial\phi_3}{\partial x_1}\phi_1 - \frac{\partial\phi_1}{\partial x_1}\phi_3\right). \end{aligned} \tag{6}$$

The above equations describe position dependencies of local polarizations, but they depend on particular APB profiles (discussed below). Here, it is worth to note an important feature, which is independent of the profile. In contrast to $P_3^{Lifshitz}$, the polarizations P_1 and P_3^{flexo} arise from total derivatives and therefore their integrals depend on the boundary conditions only (domain states 3_1 and 3_2). Then, it follows that $\langle P_1\rangle = \langle P_3^{flexo}\rangle = 0$. The total polarization $\mathcal{P}_3 = \langle P_3^{flexo} + P_3^{Lifshitz}\rangle = \langle P_3^{Lifshitz}\rangle$ is determined by the Lifshitz term only. That is important for polarization switching and interaction of the polarization with the electric field. The corresponding free energy term reads

$$-\langle P_3 E\rangle = -\langle P_3^{Lifshitz}\rangle E = -\mathcal{P}_3 E. \tag{7}$$

It means that both the occurrences of total polarization and polarization switching are fully determined by the Lifshitz term only while the flexoelectric part does not contribute to the macroscopic polarization. Here, two questions are arising, both depending on the detailed structure (i.e., profile) of the APB. The first one concerns the position dependence of the local polarization at the APB, and the second question relates to the macroscopic (total) polarization of the whole APB. Let us disclose in advance that the macroscopic polarization $\mathcal{P}_3$ is nonzero and switchable in the Néel-type APB, where $\phi_1 \neq 0$, and it is zero in the Ising-like APB. The array of the cycloidal sequence of the Néel APBs: $(3_1\uparrow 3_2\downarrow 3_1\uparrow 3_2)$, where $\uparrow$ and $\downarrow$ indicate positive or negative ϕ_1 at the APB center, respectively, yields nonzero macroscopic polarization. Applying the electric field and due to the term (7), it can be switched to the sequence $(3_1\downarrow 3_2\uparrow 3_1\downarrow 3_2)$ with opposite polarization. On the contrary, the local polarizations in the sequence $(3_1\uparrow 3_2\uparrow 3_1\uparrow 3_2)$ sum up to zero macroscopic polarization.

In order to demonstrate all above assertions, we further analyze the Ising- and Néel-type APBs. Let us start with the simplest OP profile, i.e., the Ising one $(0, 0, \phi_3) \rightarrow (0, 0, -\phi_3)$ with $\phi_3 = 0$ in the center of the DW. Then, from Eq. (4), it immediately follows $P_2 = 0$, $P_3 = 0$, and $P_1(-x_1) = -P_1(x_1)$. The asymmetric shape of $P_1(x_1)$ can be easily seen from Eq. (4), since after minimization of the free energy one arrives at $P_1 \propto \frac{\partial}{x_1}(\phi_3^2)$. These polarization components are in perfect agreement with the layer group symmetry Eq. (1) of the twin.

More complex $\mathbf{P}(x_1)$ profiles can be obtained, if we allow for an additional OP component to appear,[19] i.e., for the case of a Néel-type APB, where $(\phi_1, 0, \phi_3) \rightarrow (\phi_1, 0, -\phi_3)$. To analyze

such a situation in more detail, we use the following solution of the OP trajectory[26–28] (Fig. 4), which is valid for certain parameters of the Landau expansion

$$\phi_3 = -\frac{\phi}{2}\left[\tanh\left(\frac{x_1+\Delta}{w}\right) + \tanh\left(\frac{x_1-\Delta}{w}\right)\right],$$
$$\phi_1 = \frac{\phi}{2}\left[\tanh\left(\frac{x_1+\Delta}{w}\right) - \tanh\left(\frac{x_1-\Delta}{w}\right)\right], \tag{8}$$

where ϕ is the OP of the homogeneous DS, w is the thickness of the APB, and Δ determines roughly the half width of the layer, where ϕ_1 is about half of its maximum value. The value $\Delta = 0$ corresponds to the Ising-type wall ($\phi_1 = 0$) and $\Delta \neq 0$ to the Neél-type wall with $\phi_1 > 0$ for $\Delta > 0$ and $\phi_1 < 0$ for $\Delta < 0$.

To get an educated guess for the profiles of the polarization components, we proceed as follows. Inserting ϕ_3 and ϕ_1 from Eq. (8) into Eq. (5), we get an asymmetric profile $P_1(-x_1) = -P_1(x_1)$. Its shape is not very sensitive on the magnitudes of the coefficients W_3 and W_4, but depends on their signs, and it is independent of the sign of Δ. By way of contrast, the shape of $P_3(x_1)$ depends crucially on the coefficients W_1 and W_2. Although the full set of coefficients $W_1, .., W_4$ of the rotopolar coupling terms are not known, in Ref. 10 two of them were calculated. Since the authors were interested in ferroelastic DWs, which are at an angle of 45° with respect to the cubic main axes, they calculated the rotopolar coupling terms in a 45°-rotated system, which read

$$P_r\left(W_{rs}\frac{\partial\phi_r}{\partial s}\phi_s + W_{sr}\frac{\partial\phi_s}{\partial s}\phi_r\right), \tag{9}$$

where $\mathbf{r}$ is parallel to the domain wall, e.g., parallel to $[1\bar{1}0]$ and $\mathbf{s}$ is perpendicular to it (i.e., parallel to the DW normal $\mathbf{n} = [110]$).

The terms in Eq. (9) can be split into a flexoelectric contribution $\propto(W_{rs} + W_{sr})$ and a Lifshitz term $\propto(W_{rs} - W_{sr})$ as

$$\frac{1}{2}(W_{rs}+W_{sr})P_r\left(\frac{\partial\phi_r}{\partial s}\phi_s + \frac{\partial\phi_s}{\partial s}\phi_r\right)$$
$$+\frac{1}{2}(W_{rs}-W_{sr})P_r\left(\frac{\partial\phi_r}{\partial s}\phi_s - \frac{\partial\phi_s}{\partial s}\phi_r\right). \tag{10}$$

Transforming Eq. (3) into a 45°-rotated coordinate system by $r = \frac{1}{2}(x_1 + x_2)$ and $s = \frac{1}{2}(-x_1 + x_2)$ so that $\phi_r = \frac{1}{2}(\phi_1 + \phi_2)$ and $\phi_s = \frac{1}{2}(-\phi_1 + \phi_2)$, we obtain

$$W_{rs} = W_1 - W_2 - W_3 + W_4,$$
$$W_{sr} = W_2 - W_1 + W_4 - W_3. \tag{11}$$

In Ref. 10, it was found that $W_{rs} \gg W_{sr}$, which is consistent with $W_{sr} = W_1 - W_2 + W_4 - W_3 \approx 0$, $W_2 \gg W_1$, $W_3 \gg W_4$, and $W_2 \approx W_3$. In Fig. 4, we show the profiles (a) of $\phi_1(s)$ and $\phi_2(s)$ across the cycloidal sequence of the two ferroelastic twin boundaries $(1_1|2_1)$ and $(2_1|1_2)$ and the flexoelectric and Lifshitz contributions to the APB polarization $P_r(s)$. In agreement with the results of Ref. 10, we find a macroscopic net polarization $P_r = P_r^{flexo} + P_r^{Lifshitz} \neq 0$ of the cycloidal system of ferroelastic TBs. Also the shape, i.e., the maximum of P_r at the DW center is fully consistent with Fig. 3 of Ref. 10. Let us now check what these results imply for the polarization of a hard APB $(3_1|3_2)$, $\mathbf{n} = [100]$ of the Ising or Neél type. With the estimated parameters from above ($W_2 \gg W_1$), Eq. (5) boils down to

$$P_1 \propto W_3\frac{\partial\phi_3}{\partial x_1}\phi_3 \; P_3 \propto \frac{1}{2}(W_1+W_2)\left(\frac{\partial\phi_3}{\partial x_1}\phi_1 + \frac{\partial\phi_1}{\partial x_1}\phi_3\right)$$
$$+\frac{1}{2}(W_1-W_2)\left(\frac{\partial\phi_3}{\partial x_1}\phi_1 - \frac{\partial\phi_1}{\partial x_1}\phi_3\right) \approx W_2\frac{\partial\phi_1}{\partial x_1}\phi_3. \tag{12}$$

The shapes of P_1 and P_3 [Figs. 5(c) and 5(d)] calculated from (12) are fully consistent with the symmetry requirements (2) of the corresponding layer group. In Ref. 29, the polarization $P_3(x_1)$ of a hard APB in $SrTiO_3$ was calculated by second-principle methods. Although the values of W_1 and W_2 are not explicitly given there, the calculated double peak of $P_3(x_1)$ [Fig. 5.5(b) of Ref. 29] leads to the conclusion that for $SrTiO_3$ the condition $W_2 \gg W_1$ is indeed fulfilled. It also follows from (12) that in this case the flexoelectric term and the Lifshitz term contribute to P_3 equally. Interestingly enough, the profile of APB polarization P_3—although being symmetric in both cases—changes from peak [Fig. 4(e)] to double peak [Fig. 5(d)] for different orientations of the DW.

Such a behavior is reminiscent of the polarization profiles observed[14,15] in APBs of $PbZrO_3$ using high resolution electron microscopy. To see whether rotopolar coupling terms play an important role in lead zirconate, we will go into more details in Sec. II B.

B. Polarization of APBs in lead zirconate

$PbZrO_3$ (PZO) corresponds to the rare cases, where the polar properties of APBs have been studied[14,15] experimentally in great detail. Some of the polarization profiles [see, e.g., Figs. 4(e) and 5(c) of Ref. 14 and Fig. 1(c) of Ref. 14] resemble strikingly the double peak shape of Fig. 5(d) of the present work. We think that such double peaks are suggestive for the effect of rotopolar coupling terms. In the previous work, biquadratic coupling terms[14] were assumed to be responsible for the polarization of APBs in $PbZrO_3$. Although there is no doubt that such terms are important, it remains to check whether Lifshitz terms resembling those in $SrTiO_3$ might also be present in $PbZrO_3$.

The antiferroelectric (AFE) phase transition in lead zirconate at $T_c = 505$ K leads the crystal from the cubic perovskite phase $Pm\bar{3}m$ (Z = 1) to the orthorhombic phase $Pbam$ (Z = 8), with an eightfold multiplication of the cubic unit cell.[30,31]

The unit cell (Fig. 6) of the AFE $Pbam$ phase with lattice vectors $\mathbf{a}_o, \mathbf{b}_o, \mathbf{c}_o$ is related to the cubic phase with $\mathbf{a}_c = (a, 0, 0)$, $\mathbf{b}_c = (0, a, 0)$, *and* $\mathbf{c}_c = (0, 0, a)$ as $\mathbf{a}_o = \mathbf{a}_c - \mathbf{b}_c$, $\mathbf{b}_o = 2(\mathbf{a}_c + \mathbf{b}_c)$, and $\mathbf{c}_o = 2\mathbf{c}_c$. Note that—similar to above—all calculations are done here in the coordinate system of the cubic phase. Moreover, the origin is shifted to $(\frac{a}{2}, 0, \frac{a}{2})$ compared to the setting used for the calculations of $SrTiO_3$ from above.

The soft mode behavior[32–34] is rather complicated and involves many modes. However, the space-group symmetry change

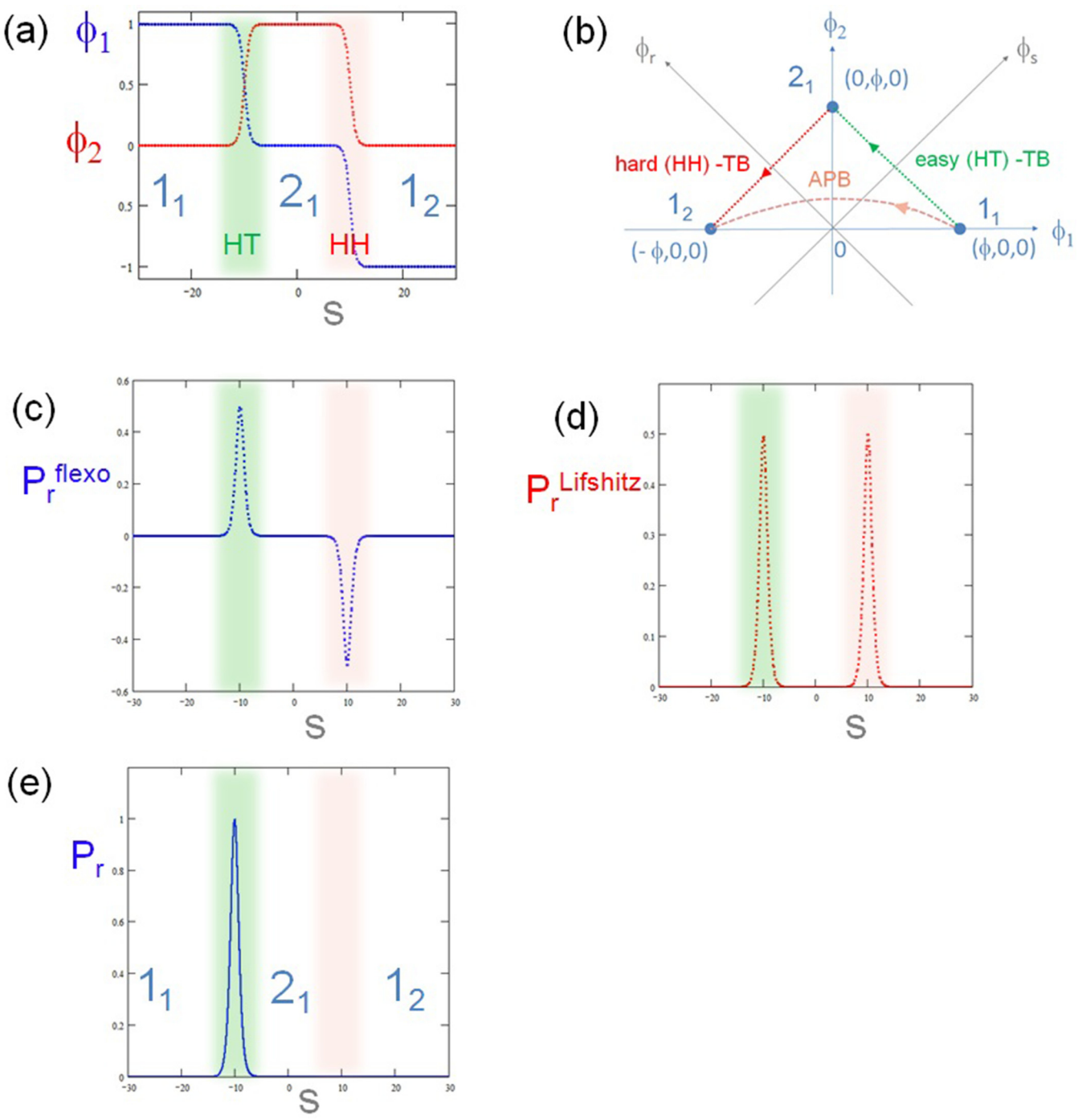

FIG. 4. Cycloidal sequence of ferroelastic twin boundaries. (a) Semi-quantitative behavior of the OP profiles $\phi_1(s)$ and $\phi_2(s)$ across the cycloidal sequence of ferroelastic TBs $(1_1|2_1)$ followed by $(2_1|1_2)$. (b) Schematics of the corresponding DW trajectories in OP space. (c) The flexoelectric contribution (10) to the polarization $P_r^{flexo}(s)$ is alternating in adjacent Domain walls, whereas (d) the Lifshitz term leads to the same polarization contribution $P_r^{Lifshitz}(s)$ in successive TBs. With the assumption of $W_2 \gg W_1$, $W_3 \gg W_4$, and $W_2 \approx W_3$ (in perfect agreement with the asymmetry $W_{rs} \gg W_{sr}$ found in Ref. 10), one obtains the macroscopic polarization contribution P_r, shown in (e).

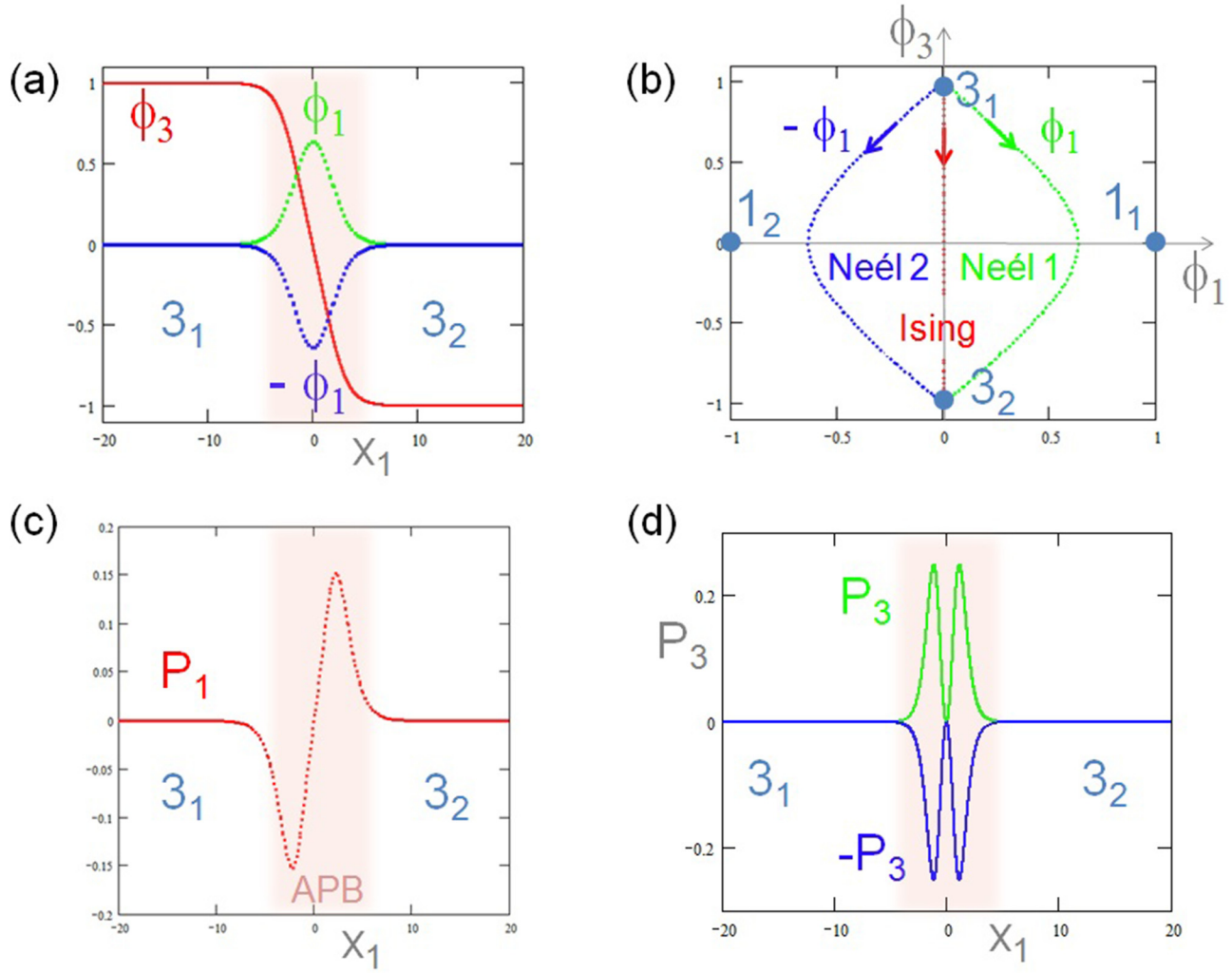

FIG. 5. Hard Neél like APB in $SrTiO_3$. Semi-quantitative behavior of (a) OP profiles ϕ_3 and ϕ_1 across a hard APB $(3_1|3_2)$, $\mathbf{n} = [100]$ and (b) OP trajectories calculated from Eq. (8) with $\phi = 1$, $w = 2$, $\Delta = 1.5$. Note that the trajectories Neél 1 and Neél 2 correspond to $\Delta = 1.5$ and $\Delta = -1.5$, respectively. The corresponding polarization profile for the component P_1 perpendicular to the APB is shown in (c). Its asymmetric shape is in perfect agreement with the layer group (2) under the assumption of $\phi_1 \neq 0$. Panel (d) shows the component P_3 within the domain wall. It was calculated from Eqs. (8) and (12) with the assumption $W_2 \gg W_1$. The double peak profile is in perfect agreement with the results [Fig. 5.5(b)] of Ref. 29.

can be well understood[35,36] as a result of the condensation of two order parameters. The lead displacements are described by the condensation of a wave with a propagation vector $\mathbf{k}_\Sigma = \frac{2\pi}{a}(\frac{1}{4}, \frac{1}{4}, 0)$. The corresponding OP η_i, $(i = 1, 12)$ transforms according to the 12-dimensional irreducible representation[37] Σ_2. In the first orientational domain state (DS), the equilibrium order parameter is given by $(\eta, -\eta, 0, 0, 0, 0, 0, 0, 0, 0, 0, 0)$. A condensation of the Σ_2-mode alone would lead[36] to a *Pbam* phase, however, with a change of the unit cell volume by a factor of 4, i.e., without doubling of the unit cell in the *c*-direction. To get the unit cell doubling in the *c*-direction, one has to take into account the antiphase rotations of the oxygen octahedra, which are described by the condensation of a wave with $\mathbf{k}_R = \frac{2\pi}{a}(\frac{1}{2}, \frac{1}{2}, \frac{1}{2})$, with order parameter components (ϕ_1, ϕ_2, ϕ_3) transforming under the irrep R_4^+, as in $SrTiO_3$. The equilibrium OP that describes the first DS is given for $PbZrO_3$ as $(\phi, \phi, 0)$.

The symmetry breaking $Pm\bar{3}m(V) \rightarrow Pbam(8V)$ leads to $48/8 \times 8 = 48$ DSs. We do not intend here to perform a complete symmetry analysis of domains and domain twins in $PbZrO_3$ as we have done for $SrTiO_3$. A detailed symmetry analysis of PZO will be given elsewhere. Here, we want to focus on a few selected APBs, which have been investigated in very detail experimentally, as well as by computer simulations and the Landau theory.[14,15] Since the condensation of Σ_2 is associated with a fourfold increase in the

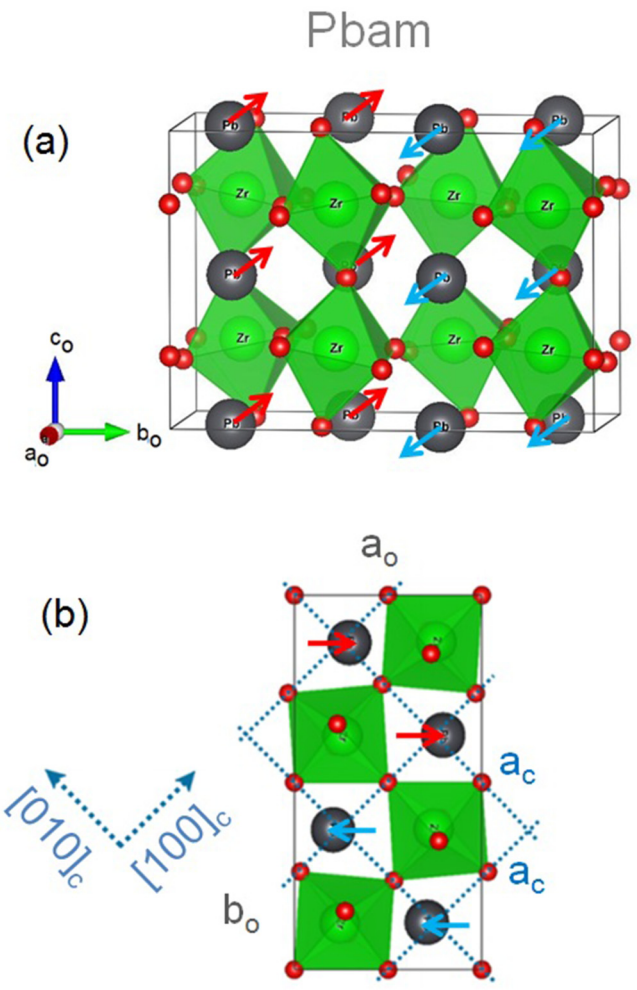

FIG. 6. Structure of $PbZrO_3$. (a) Crystal structure of the *Pbam* unit cell of $PbZrO_3$. (b) Projection of the *Pbam* structure onto the (x, y) plane. The arrows indicate the displacements of the Pb cations in the Σ_2 mode. These Pb displacements along the pseudocubic $[1\bar{1}0]$ direction can be written[14] as $\mathbf{r}_{Pb} \propto (1, -1, 0)\cos\left(\frac{\pi}{2a_c}(x_c + y_c) + \varphi\right)$.

number of atoms in the unit cell, every orientational DS can exist in four different translational DSs with respect to lead displacements.[38] We denote them as

$$\begin{aligned} 1_1 &= (\eta, -\eta, 0, 0, 0, 0, 0, 0, 0, 0, 0, 0), \\ 1_2 &= (-\eta, -\eta, 0, 0, 0, 0, 0, 0, 0, 0, 0, 0), \\ 1_3 &= (-\eta, \eta, 0, 0, 0, 0, 0, 0, 0, 0, 0, 0), \\ 1_4 &= (\eta, \eta, 0, 0, 0, 0, 0, 0, 0, 0, 0, 0). \end{aligned} \tag{13}$$

The translational DSs within a given orientational state can be transformed from one to another by shifting the lattice, e.g., by $(a, 0, 0)$, $(2a, 0, 0)$, or $(3a, 0, 0)$, which after application of the matrix element $(1|t_1, t_2, t_3)$, $(t_1 = na, t_2 = ma, t_3 = la)$ of the irrep Σ_2 leads to the identification

$$\begin{aligned} 1_1 - (\mathbf{a_c}, \pi/2) &\rightarrow 1_2, \\ 1_1 - (2\mathbf{a_c}, \pi) &\rightarrow 1_3, \\ 1_1 - (3\mathbf{a_c}, 3\pi/2) &\rightarrow 1_4. \end{aligned} \tag{14}$$

For these three types of APBs, i.e., $(1_1|1_2)$, $(1_1|1_3)$, and $(1_1|1_4)$, the corresponding lead displacements differ in phases of $\Delta\varphi = \pi/2, \pi$, and $3\pi/2$, respectively (Fig. 7).

Figure 8 shows the polarization profiles $P_x(y)$ and $P_y(y)$ of PZO of two π-APBs, reproduced from Fig. 4(e) of Ref. 14 and Figs. 2(e) and 2(f) of Ref. 15. It should be noted that in the work of Wei *et al.*[14,15] the used axes for the polarization $P_x(y)$, $P_y(y)$, as well as the displacement vectors **R** and DW normal **n** are given in the orthorhombic coordinate system, which is rotated by 45° around the z-axis of the cubic coordinate system. For these APBs, the adjacent domain states differ by the same displacement vector $\mathbf{R} = \frac{1}{4}[02n]$ with $n = 0$ or $n = 2$, which in the cubic reference system corresponds to $(a, a, 0)$ or (a, a, a) for $n = 0$ or $n = 2$, respectively. Since this is equivalent to $(2a, 0, 0)$, $(2a, 0, a)$, the corresponding APB is of the π type. In our notation, the APBs shown in Fig. 8 correspond to a domain pair $(1_1|1_3)$ (Fig. 7) with normal vector $\mathbf{n} = [010]$ and different DW centers. Thus, $P_x(y)$ denotes the in-plane polarization profile, and $P_y(y)$ describes the variation

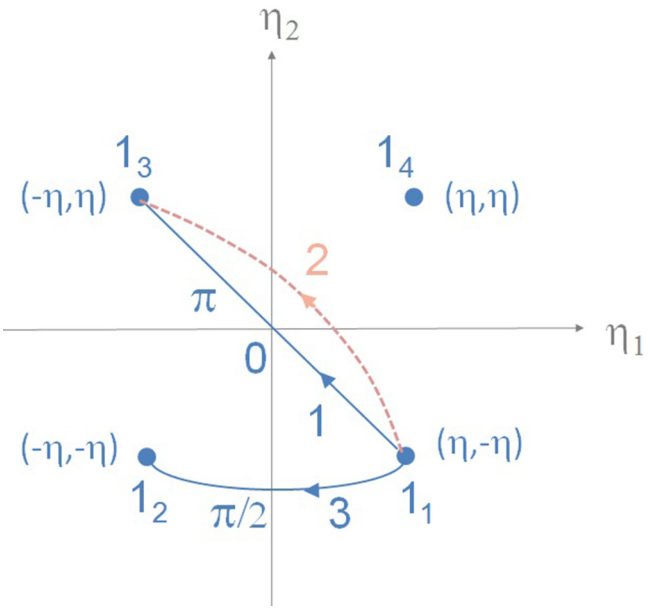

FIG. 7. Translational DSs and APBs in OP space. Mapping of the translational domain states and APBs within a single orientational DS of $PbZrO_3$ in the subspace (η_1, η_2) of the OP space $\boldsymbol{\eta}$. Circles represent the four different domain states 1_1, 1_2, 1_3, 1_4, and lines describe some possible pathways of the corresponding APB in the OP space; e.g., line 1 represents an Ising wall between 1_1 and 1_3, and line 2 is a Neél wall of the corresponding domain pair.

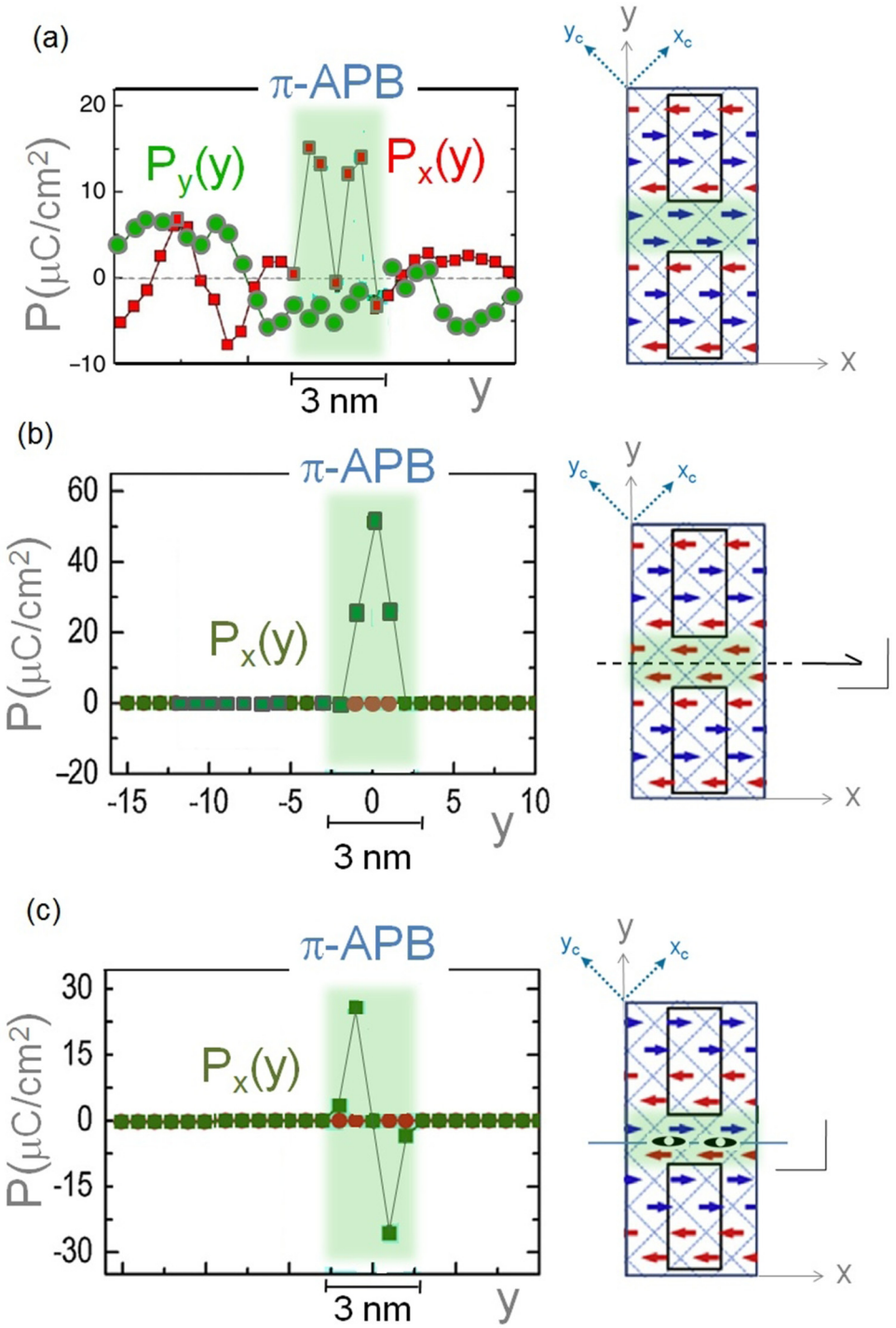

FIG. 8. Polarization profiles of APBs in PZO.[14,15] (a) Dipole moment densities[14] P_x and P_y of an APB with a displacement vector $\mathbf{R} = \frac{1}{4}[02n]$ in $PbZrO_3$. The right-hand side shows a sketch of the APB with normal n = [010] (from Fig. 1 of Ref. 15). (b) Polarization profile for an APB with $\mathbf{R} = \frac{1}{4}[02n]$ with DW center at $\mathbf{p} = (0, \sqrt{2}a/2, 0)$ (axes are in the orthorhombic *Pabm* coordinate system). The layer group symmetry [Eq. (15)] (see also symbols at the right-hand side) is polar. (c) Polarization profile for an APB with the same displacement vector as in (a) and (b) but with DW center at $\mathbf{p} = (0, 0, 0)$. In this case, the layer group symmetry Eq. (16) (see the right-hand side) is not polar. In all these cases, the phase shift of the lead displacements of adjacent antiphase domains is $\Delta\varphi = \pi$. They differ only in their position of the DW center.

of the perpendicular (to the APB) component along the DW normal.

There is an ambiguity in the DW structure corresponding to Fig. 8(a), which is originally shown in Fig. 1 of Ref. 15. In our opinion, such a local structure is not possible for an infinitely thin APB and we will therefore not analyze it further here.

The symmetry elements of the layer groups corresponding to the two other π-APBs [Figs. 8(b) and 8(c)] in PZO are, for the DW center at position $\mathbf{p} = (0, \sqrt{2}a/2, 0)$ [corresponding to $\mathbf{p} = (a/2, a/2, 0)$ in the shifted cubic coordinate system],

$$T_{1_1 1_3} = \mathbf{T}\Big\{(1/000)\,(m_z/000)\,(\underline{\hat{m}}_{xy}/\frac{a}{2}-\frac{a}{2}0)\,(\underline{\hat{2}}_{\bar{x}y}/\frac{a}{2}-\frac{a}{2}0)\Big\}, \quad (15)$$

with $\mathbf{T} = (na, -na, 2ma)$. This polar symmetry allows for the development of an even in-plane polarization component $P_x(-y) = P_x(y)$ [Fig. 8(b)]. The other two components are constrained by this symmetry to $P_y(-y) = -P_y(y)$ and $P_z(y) \equiv 0$, in perfect agreement with the results of Wei *et al.*[14,15] For the other position of the DW center [$\mathbf{p} = (0, 0, 0)$] in Fig. 8(c), the layer group consists of the following symmetry elements:

$$T_{1_1 1_3} = \mathbf{T}\{(1/000)\,(m_z/000)\,(\underline{\hat{2}}_z/000)\,(\underline{\hat{\bar{1}}}/000)\}. \quad (16)$$

This non-polar group implies $P_x(-y) = -P_x(y)$, $P_y(-y) = -P_y(y)$, and $P_z(y) \equiv 0$, which agrees also perfectly with the polarization profiles of Ref. 15.

To check whether similar Lifshitz terms like in $SrTiO_3$ exist for $PbZrO_3$, we have used the irreps Σ_2 to calculate all possible invariants of the type $W_{ijkl}P_i\eta_k\frac{\partial\eta_l}{\partial x_j}$. Taking only the part which is relevant for the observed polarization profiles, the whole set of invariants boils down to

$$W_0 = P_x\left[\frac{\partial}{\partial y}(\eta_1^2+\eta_2^2)\right] + P_y\left[\frac{\partial}{\partial x}(\eta_1^2+\eta_2^2)\right]. \quad (17)$$

In the 45°-rotated coordinate system given by $\tilde{x} = \frac{1}{\sqrt{2}}(x+y)$ and $\tilde{y} = \frac{1}{\sqrt{2}}(-x+y)$, this reads

$$W_0 = P_{\tilde{x}}\left[\frac{\partial}{\partial \tilde{x}}(\eta_1^2+\eta_2^2)\right] - P_{\tilde{y}}\left[\frac{\partial}{\partial \tilde{y}}(\eta_1^2+\eta_2^2)\right]. \quad (18)$$

Since the OP components η_1, η_2 vary with $\tilde{y}$, it is evident that these invariants cannot lead to an in-plane polarization $P_{\tilde{x}} \propto \frac{\partial}{\partial \tilde{x}}(\eta_1^2+\eta_2^2)$.

To go a step further, we have calculated higher order invariants, i.e., of the type $\propto P_i\eta_j\eta_k\frac{\partial}{\partial x_l}(\eta_m\eta_n)$. Among the large number of such invariants (remember the 12 component OP), the most promising term is of the form

$$W_1 = P_x\left[\eta_1\eta_2\frac{\partial}{\partial y}(\eta_3\eta_4) - \eta_3\eta_4\frac{\partial}{\partial y}(\eta_1\eta_2)\right] + P_y\left[\eta_3\eta_4\frac{\partial}{\partial x}(\eta_1\eta_2) - \eta_1\eta_2\frac{\partial}{\partial x}(\eta_3\eta_4)\right], \quad (19)$$

which after transformation to the rotated coordinate system $\tilde{\mathbf{x}}$ takes exactly the same form as Eq. (19), only $\mathbf{x}$ is replaced by $\tilde{\mathbf{x}}$. Then, we would get for an APB with $\mathbf{n} = [\bar{1}10]$

$$P_{\tilde{x}}(\tilde{y}) \propto \eta_1\eta_2\frac{\partial}{\partial \tilde{y}}(\eta_3\eta_4) - \eta_3\eta_4\frac{\partial}{\partial \tilde{y}}(\eta_1\eta_2),$$
$$P_{\tilde{y}}(\tilde{y}) = 0, \quad P_z(\tilde{y}) = 0. \quad (20)$$

$P_{\tilde{x}}(\tilde{y}) = 0$ because the OP components do not vary with $\tilde{x}$, and $P_z(\tilde{y})$ vanishes because there is no higher order coupling to P_z.

From Eq. (20), it is clear that this coupling mechanism can lead to an in-plane polarization of an APB in $PbZrO_3$ only if in addition to the components η_1, η_2 the components η_3, $\eta_4 \neq 0$. Bearing in mind that the symmetry operation $(4_z^+|000)$ transforms the domain state $1_1 = (\eta, -\eta, 0, 0, 0, 0, 0, 0, 0, 0, 0, 0)$ to the orientational domain state $2_1 = (0, 0, -\eta, \eta, 0, 0, 0, 0, 0, 0, 0, 0)$, one realizes that η_3, $\eta_4 \neq 0$ implies that in the corresponding APB $(1_1|1_2)$ or $(1_1|1_3)$, etc., the OP must pass via a nucleus of a ferroelastic domain 2_1. This scenario which finally is very similar to the case of $SrTiO_3$ will be worked out in a forthcoming paper.

III. SUMMARY AND CONCLUSIONS

In the present work, we have analyzed the polar properties of translational antiphase boundaries (APBs) of $SrTiO_3$ (STO) and $PbZrO_3$ (PZO). We used a method[12] based on the well-known layer group analysis of domains and domain twins,[24] which we combined with order parameters and the Landau theory to get a clue on the polarization profiles of the corresponding APBs. Using this extension of the classical crystallographic layer group approach, one can study the properties of domain walls even if one allows for the appearance of additional (to the spontaneous ones) order parameter components to occur within the wall. It turns out, in agreement with the results of Refs. 19 and 22, that hard APBs in $SrTiO_3$ can carry a symmetric in-plane polarization. We also found that in addition to the bi-quadratic $P^2\phi^2$ terms in the corresponding Landau free energy antisymmetric Lifshitz terms between the polarization and gradients of the oxygen octahedra rotations exist, which lead to polarization profiles that are fully compatible with the present layer group results as well as with recent computer simulations.[29] Moreover, it turns out that the same Lifshitz terms determine the polarization of a cycloidal sequence[34] of 90° ferroelastic domain walls. Such DW polarization induced by Lifshitz terms can be switched by the application of an external electric field, which makes it very interesting for nanotechnological applications.

In $PbZrO_3$, the situation is more complicated. The structural changes from $Pm\bar{3}m(V) \rightarrow Pbam(8V)$ cannot be described by a single order parameter.[32,33] For a given orientational domain state, a combination of two order parameters describes the displacement pattern in the distorted phase. One corresponding to the Σ_2 representation at $\mathbf{k}_\Sigma = (2\pi/a)(1/4, 1/4, 0)$ with OP components $\eta_i (i = 1\text{–}12)$ describes mainly the displacements of lead ions, whereas the R_4^+-mode at $\mathbf{k}_R = (2\pi/a)(1/2, 1/2, 1/2)$ with OP components $\phi_i (i = 1-3)$ is related to antiphase rotations of the oxygen octahedra.[36] $PbZrO_3$ is a very nice example, where polarization profiles[14,15] of APBs have been experimentally determined. The shapes of these profiles depend crucially on the position of the

domain wall centers; e.g., for some of them symmetric in-plane polarization is possible, whereas for others only asymmetric ones are measured.[14,15] This behavior—which reflects the fact that the macroscopic symmetry (point group) of a translational APB can depend on the position of the domain wall center[12,39]—is fully described within the present layer group analysis of APBs in $PbZrO_3$. A systematic symmetry analysis excludes the existence of asymmetric Lifshitz terms of the type $P_i\eta_j\partial\eta_k/\partial x_i$ for PZO, but leaves a number of Lifshitz-like invariants of higher order type representing promising candidates for understanding the polarization pattern of APBs in $PbZrO_3$.

ACKNOWLEDGMENTS

This work was supported by the Austrian Science Fund (FWF) under Grant No. P28672-N36.

DATA AVAILABILITY

The data that support the findings of this study are available from the corresponding author upon reasonable request.

REFERENCES

[1]T. Sluka, A. K. Tagantsev, P. Bednyakov, and N. Setter, Nat. Commun. **4**, 1808 (2013).
[2]S. Van Aert, S. Turner, R. Delville, D. Schryvers, G. Van Tendeloo, and E. K. H. Salje, Adv. Mater. **24**, 523 (2012).
[3]H. Yokota, H. Usami, R. Haumont, P. Hicher, J. Kaneshiro, E. K. H. Salje, and Y. Uesu, Phys. Rev. B. **89**, 144109 (2014).
[4]H. Yokota, S. Niki, R. Haumont, P. Hicher, and Y. Uesu, AIP Adv. **7**, 085315 (2017).
[5]G. Catalan, J. Seidel, R. Ramesh, and J. F. Scott, Rev. Mod. Phys. **84**, 119 (2012).
[6]E. K. H. Salje, O. Aktas, M. A. Carpenter, V. V. Laguta, and J. F. Scott, Phys. Rev. Lett. **111**, 247603 (2013).
[7]E. K. H. Salje, M. Alexe, S. Kustov, M. C. Weber, J. Schiemer, G. F. Nataf, and J. Kreisel, Sci. Rep. **6**, 1 (2016).
[8]H. Yokota, N. Hasegawa, M. Glazer, E. K. H. Salje, and Y. Uesu, Appl. Phys. Lett. **116**, 232901 (2020).
[9]Y. Gu, M. Li, A. N. Morozovska, Y. Wang, V. Gopalan, and L.-Q. Chen, Phys. Rev. B **89**, 174111 (2014).
[10]A. Schiaffino and M. Stengel, Phys. Rev. Lett. **119**, 137601 (2017).
[11]W. Schranz, C. Schuster, A. Tröster, and I. Rychetsky, "Polarization of domain boundaries in $SrTiO_3$ studied by layer group and order parameter symmetry," Phys. Rev. B **102**, 184101 (2020).
[12]W. Schranz, I. Rychetsky, and J. Hlinka, Phys. Rev. B **100**, 184105 (2019).
[13]A. N. Morozovska, E. A. Eliseev, M. D. Glinchuk, L. Q. Chen, and V. Gopalan, Phys. Rev. B. **85**, 094107 (2012).
[14]X. K. Wei, A. K. Tagantsev, A. Kvasov, K. Roleder, C. L. Jia, and N. Setter, Nat. Commun. **5**, 3031 (2014).
[15]X. K. Wei, C. L. Jia, K. Roleder, and N. Setter, Mater. Res. Bull. **62**, 101 (2015).
[16]S. Lei, H. Fan, J. Fang, X. Ren, L. Ma, and H. Tian, Inorg. Chem. Front. **5**, 568 (2018).
[17]G. F. Nataf, M. Guennou, J. M. Gregg, D. Meier, J. Hlinka, E. K. H. Salje, and J. Kreisel, Nat. Rev. Phys. **2**, 662 (2020).
[18]S. Fukami, V. O. Lorenz, and O. Gomonai, J. Appl. Phys. **128**, 070401 (2020).
[19]A. K. Tagantsev, E. Courtens, and L. Arzel, Phys. Rev. B **64**, 224107 (2001).
[20]K. Momma and F. Izumi, "VESTA 3 for three-dimensional visualization of crystal, volumetric and morphology data," J. Appl. Crystallogr. **44**, 1272–1276 (2011).
[21]H. Unoki and T. Sakudo, J. Phys. Soc. Jpn. **23**, 546 (1967).
[22]A. Kvasov, A. K. Tagantsev, and N. Setter, Phys. Rev. B **94**, 054102 (2016).
[23]R. Wang, Y. Zhu, and S. M. Shapiro, Phys. Rev. B **61**, 8814 (2000).
[24]V. Janovec and J. Přívratská, in *International Tables for Crystallography*, edited by A. Authier (Wiley, New York, 2006), Vol. D, Chaps. 3–4, pp. 449–505.
[25]B. Houchmanzadeh, J. Lajzerowicz, and E. Salje, J. Phys. Condens. Matter **3**, 5163 (1991).
[26]Y. Ishibashi and V. Dvorak, J. Phys. Soc. Jpn. **41**, 1650 (1976).
[27]E. B. Sonin and A. K. Tagantsev, Ferroelectrics **98**, 291 (1989).
[28]A. A. Bullbich and Yu. M. Gufan, Ferroelectrics **98**, 277 (1989).
[29]C. Escorihuela-Sayalero, "Second-principle methods for large-scale simulations of realistic functional oxides," Ph.D. thesis (University of Luxembourg, 2019).
[30]H. Fujishita and S. Hoshino, J. Phys. Soc. Jpn. **53**, 226 (1984).
[31]H. Fujishita and S. Katano, J. Phys. Soc. Jpn. **66**, 3484 (1997).
[32]A. K. Tagantsev, K. Vaideeswaran, S. B. Vakhrushev, A. V. Filimonov, R. G. Burkovsky, A. Shaganov, D. Andronikova, A. I. Rudskoy, A. Q. R. Baron, H. Uchiyama, D. Chernyshov, A. Bosak, Z. Ujma, K. Roleder, A. Majchrowski, J.-H. Ko, and N. Setter, Nat. Commun. **4**, 2229 (2013).
[33]J. Hlinka, T. Ostapchuk, E. Buixaderas, C. Kadlec, P. Kuzel, I. Gregora, J. Kroupa, M. Savinov, A. Klic, J. Drahokoupil, I. Etxebarria, and J. Dec, Phys. Rev. Lett. **112**, 197601 (2014).
[34]J. Íñiguez, M. Stengel, S. Prosandeev, and L. Bellaiche, Phys. Rev. B **90**, 220103 (R) (2014).
[35]K. M. Rabe, in *Functional Metal Oxides: New Science and Novel Applications*, edited by S. Ogale and V. Venkateshan (Wiley, Hoboken, NJ, 2013).
[36]P. Tolédano and D. D. Khalyavin, Phys. Rev. B **99**, 024105 (2019).
[37]M. I. Aroyo, A. Kirov, C. Capillas, J. M. Perez-Mato, and H. Wondratschek, "Bilbao crystallographic server II: Representations of crystallographic point groups and space groups," Acta Crystallogr. A **62**, 115–128 (2006).
[38]The translational domain states with respect to the oxygen octahedra rotations $\boldsymbol{\phi}$ are not considered in the present work.
[39]V. Janovec, W. Schranz, H. Warhanek, and Z. Zikmund, Ferroelectrics **98**, 171 (1989).